

Electronic supplementary information for

Competition between electron transfer, trapping, and recombination in CdS nanorod-hydrogenase complexes

James K. Utterback,^a Molly B. Wilker,^a Katherine A. Brown,^b Paul W. King,^b Joel D. Eaves,^a and Gordana Dukovic*^a

^a Department of Chemistry and Biochemistry, University of Colorado Boulder, Boulder, Colorado 80309, USA. E-mail: gordana.dukovic@colorado.edu

^b Biosciences Center, National Renewable Energy Laboratory, Golden, Colorado 80401, USA

Table of Contents

I.	Sample preparation and characterization	S2
II.	Transient absorption (TA) spectroscopy	S2
III.	TA spectra of CdS nanorods	S3
IV.	Fitting of TA kinetics	S3
V.	The kinetic model for excited state relaxation in NRs and CdS–CaI complexes	S4
VI.	Fluctuations in both numbers and intrinsic rate constants for traps and CaI	S6
VII.	Error Analysis for k_0 , $\langle N_{tr} \rangle$, k_{tr} , $\langle N_{CaI} \rangle$ and k_{ET}	S8
VIII.	Kinetic modeling of another CdS–CaI dataset	S9
IX.	QE_{ET} as a function of the intrinsic rate constants	S10
X.	References	S11

I. Sample preparation and characterization

The synthesis of CdS nanorods (NRs) was carried out following previously reported methods.¹⁻³ UV-visible absorption spectra were recorded at room temperature in 2 mm quartz cuvettes using an Agilent 8453 spectrophotometer equipped with tungsten and deuterium lamps (Fig. S1a). The sizes of the NRs were determined by measuring over 200 particles in TEM images (Fig. S1b) using ImageJ software,⁴ giving an average length of 21.5 ± 5.2 nm and an average diameter of 4.4 ± 0.6 nm. TEM samples were made by drop casting CdS NR solution onto 300 mesh, copper grids with carbon film from Electron Microscopy Science. Images were taken using a Phillips CM100 TEM at 80 kV with a bottom-mounted 4 megapixel AMT v600 digital camera.

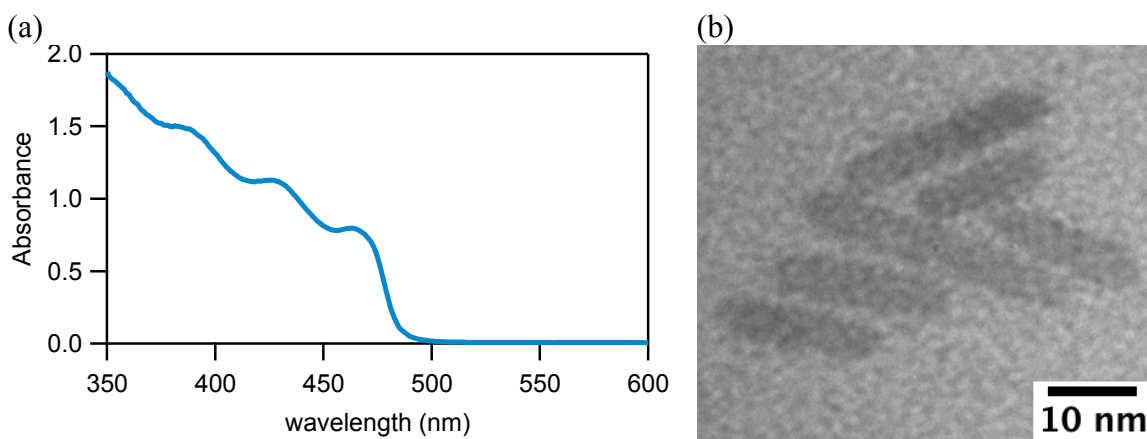


Fig. S1. (a) UV-visible absorption spectrum of CdS NRs in buffer. (b) TEM image of CdS NRs.

CdS NR surfaces were functionalized, subsequent to NR synthesis, with 3-mercaptopropanoic acid (3-MPA) using a previously reported ligand exchange procedure.^{2, 3, 5} This enabled aqueous solubility and an electrostatic interaction with CaI. The molar absorptivity of the CdS NRs was found by comparison of UV-visible absorption spectra (Fig. S1) with Cd²⁺ concentrations, found by elemental analysis (ICP-OES), after acid digestion of NR samples. The estimated molar absorptivity at 350 nm was 1.1×10^7 M⁻¹ cm⁻¹ for this sample. The expression and purification of CaI from *Escherichia coli* has been described elsewhere.⁶ CdS–CaI complexes were prepared under Ar by mixing solutions of CdS NRs and CaI in buffer (50 mM Tris-HCl, 5 mM NaCl, 5% glycerol, pH 7) with no hole scavenger added.

II. Transient absorption (TA) spectroscopy

The complete experimental setup for the TA measurements has been previously described.³ In all mixtures used for TA experiments, the concentration of CdS was held constant at about 0.7 μ M, as determined from UV-visible absorption spectra and the molar absorptivity, and the concentration of CaI was varied relative to this in order to give different molar ratios CaI:CdS. Samples were sealed under Ar in 2 mm quartz cuvettes equipped with air-tight valves. TA samples were rapidly stirred and pumped with a beam that was ~ 240 μ m in diameter with pulse energies of ~ 10 nJ. The pump power was low enough that TA decay kinetics were independent of power to prevent signal from multiple excitons⁷ and isolate the kinetics of one electron transferring to CaI. TA kinetics for data sets in Fig. 1, 2 and S5 were taken with a time resolution of 0.3 ns.

III. TA spectra of CdS nanorods

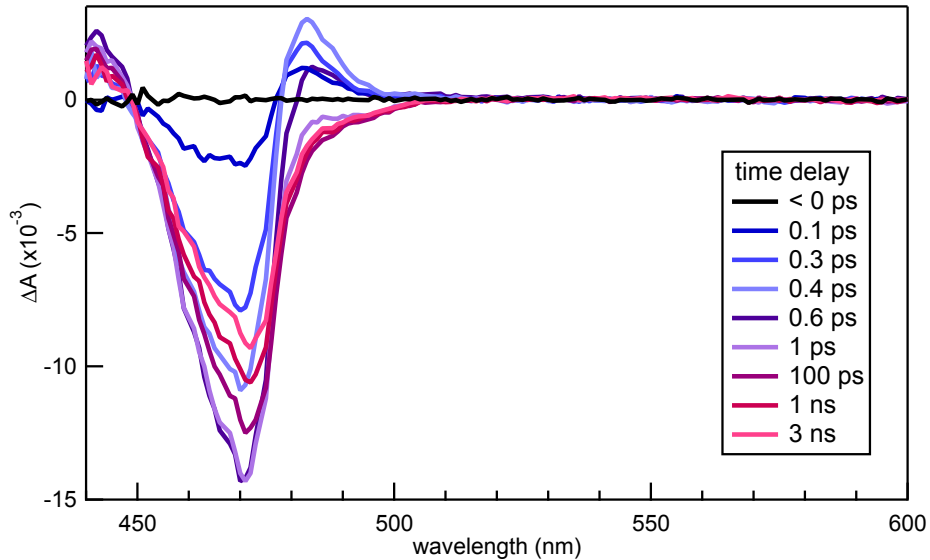


Fig. S2. TA spectra of CdS NRs after 400 nm excitation at various time delays. Photoexcitation of CdS NRs at 400 nm gives rise to a transient bleach feature peaked at 471 nm in this particular sample, corresponding the band gap. Kinetic traces are obtained by monitoring the ΔA amplitude at 471 nm. The induced absorption feature at 485 nm is due to carrier cooling and is short lived (< 1 ps).

IV. Fitting of TA kinetics

The TA decay over the time span of 0.1 ps – 30 μ s (Fig. S3) has three time windows with distinct decay shapes.

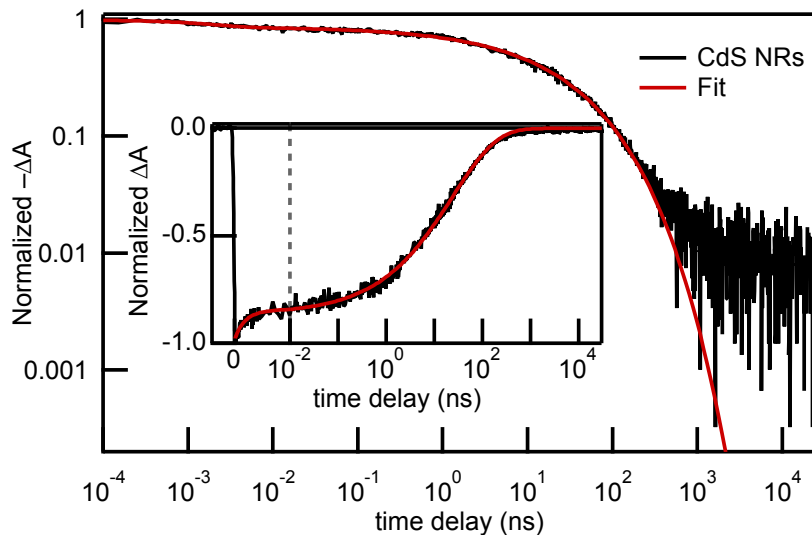


Fig. S3. TA kinetics of the band gap feature in CdS NRs probed at 471 nm over a time window of 0.1 ps–30 μ s with a time resolution of 150 fs. The signal is shown as $-\Delta A$ on log-log axes. The inset shows the same data on a split time axis that is linear for the first 10 ps and logarithmic thereafter. A fit function that includes a fast single exponential plus a stretched exponential is shown in red. The plots reveal the existence of three time windows with distinct functional forms.

The decay can be broken up into short (0.1–10 ps), intermediate (10 ps – 100 ns) and long (100 ns – 30 μ s) time windows, where each time window has a different functional

form. The single exponential plus a stretched exponential fit function used in to fit the TA band edge bleach decay of CdS NRs in Fig. S3 is

$$f(t) = A_{\text{exp}} e^{-t/\tau_{\text{exp}}} + A_{\text{stretch}} e^{-(t/\tau_{\text{stretch}})^\beta}. \quad (\text{Eq. S1})$$

The resulting fit parameters by applying Eq. S1 are $A_{\text{exp}} = -0.12$, $\tau_{\text{exp}} = 1.8$ ps, $A_{\text{stretch}} = -0.88$, $\tau_{\text{stretch}} = 24$ ns and $\beta = 0.47$. The fast 1.8 ps single exponential decay component constitutes 12% of the overall decay and has been attributed to exciton localization to a part of the nanorod with the largest diameter, or weakest quantum confinement.⁸ Most of the decay (86%) occurs in the intermediate time window and can be described with a stretched exponential with a time constant of 24 ns and a stretching exponent of 0.47. There is also a long-lived component that makes up about 2% of the ΔA amplitude that is not described by the stretched exponential fit. The origin of this component is not understood and not addressed here.

In this communication, we focus on the 1-100 ns time range because most of the TA signal change associated with ET occurs within this range.⁹ The fit to Eq. 2 produces similar parameter values to those in Table 1 when we expand the range to 0.01-100 ns.

V. The kinetic model for excited state relaxation in NRs and CdS–CaI complexes

For completeness, we present the derivation of the model of the CdS survival probability, $P_{\text{CdS}}(t)$. Though this derivation closely follows previously published works,¹⁰ it is a foundational part of our description for electronic relaxation in the presence of both traps and enzyme with and without rate constant fluctuations (Section VII).

The TA signal is proportional to the number of electrons in the $1\sigma_e$ excited state at time t , which is the survival probability of the electron in excited state, $P_{\text{CdS}}(t)$, multiplied by the total number of electrons excited at time zero. Thus the survival probability fully characterizes the time-dependent relaxation embodied in the TA signal, $\Delta A(t)$. The total survival probability, $P_{\text{CdS}}(t)$, is related to the conditional survival probability for a NR that has a given number N_{tr} of traps, $P_{\text{CdS}}(t, N_{\text{tr}})$, by the law of total probability $P_{\text{CdS}}(t) = \sum_{N_{\text{tr}}=0}^{\infty} P(N_{\text{tr}}) P_{\text{CdS}}(t, N_{\text{tr}})$. Because each NR is independent, one can view $P_{\text{CdS}}(t, N_{\text{tr}})$ as the total number of electrons in the excited state at time t divided by the total number of electrons that were excited at time zero for the subpopulation where N_{tr} is fixed. $P(N_{\text{tr}})$ is the (time-independent) probability that one NR has N_{tr} traps and can be computed from equilibrium statistical mechanics. The equation of motion for $P_{\text{CdS}}(t, N_{\text{tr}})$ is the master equation,¹¹

$$\frac{dP_{\text{CdS}}(t, N_{\text{tr}})}{dt} = -(k_0 + k_{\text{tr}} N_{\text{tr}}) P_{\text{CdS}}(t, N_{\text{tr}}). \quad (\text{Eq. S2})$$

The factor of $k_{\text{tr}} N_{\text{tr}}$ is the total probability, per unit time, that an electron reacts with *any* of the N_{tr} traps. The rate constant k_0 is the probability per unit time that the electron relaxes by any process other than trapping. This model assumes that the photophysics occurs in the “well-mixed” limit, i.e., that the electron samples the spatial extent of the NR on a timescale that is fast compared to the trapping time. This means that the time required for an electron to find a trap is not dominated by diffusion in this time window. The solution to Eq. S2 is

$$P_{\text{CdS}}(t, N_{\text{tr}}) = P_{\text{CdS}}(t_0, N_{\text{tr}})e^{-(k_0+k_{\text{tr}}N_{\text{tr}})(t-t_0)}. \quad (\text{Eq. S3})$$

The survival probability decays in the short time window (0.1 ps – 10 ps) in a way that is independent of N_{tr} ⁸ so that the initial condition becomes $P_{\text{CdS}}(t_0, N_{\text{tr}}) = P_{\text{CdS}}(t_0)$, the amplitude at time t_0 after the relaxation of CdS between time 0 and t_0 .

We describe the distribution of electron trap sites, $P(N_{\text{tr}})$, as an ensemble of NRs coupled to an ideal solution of traps that are noninteracting with one another but are at fixed chemical potential, temperature and volume so that the number of traps at equilibrium, N_{tr} , in a NR follows a Poisson distribution:

$$P(N_{\text{tr}}) = \frac{\langle N_{\text{tr}} \rangle^{N_{\text{tr}}} e^{-\langle N_{\text{tr}} \rangle}}{N_{\text{tr}}!}. \quad (\text{Eq. S4})$$

where $\langle N_{\text{tr}} \rangle$ is the average number of traps at thermal equilibrium. The decay of the ensemble of complexes, $P_{\text{CdS}}(t)$, computed from probability theory is then equivalent to a thermal ensemble average,

$$P_{\text{CdS}}(t) = \sum_{N_{\text{tr}}=0}^{\infty} P(N_{\text{tr}})P_{\text{CdS}}(t, N_{\text{tr}}), \quad (\text{Eq. S5})$$

$$= P_{\text{CdS}}(t_0)e^{-k_0 t} \left[\sum_{N_{\text{tr}}=0}^{\infty} P(N_{\text{tr}})e^{-k_{\text{tr}}N_{\text{tr}}t} \right], \quad (\text{Eq. S6})$$

$$= P_{\text{CdS}}(t_0) \exp\{-k_0(t - t_0) + \langle N_{\text{tr}} \rangle(e^{-k_{\text{tr}}(t-t_0)} - 1)\}. \quad (\text{Eq. S7})$$

Because $k_0 t_0 \ll 1$ and $k_{\text{tr}} t_0 \ll 1$, we simplify the fit equation by omitting t_0 and writing $P_{\text{CdS}}(t_0)$ as the amplitude, a_{CdS} :

$$P_{\text{CdS}}(t) = a_{\text{CdS}} \exp\{-k_0 t + \langle N_{\text{tr}} \rangle(e^{-k_{\text{tr}}t} - 1)\}. \quad (\text{Eq. S8})$$

This is the model (Eq. 2) we use to describe the TA decay kinetics in Fig. 1.

We arrive at Eq. 3 in the manuscript starting with a model for the conditional survival probabilities for photoexcited electrons in CdS NRs with both traps and adsorbed CaI moieties, $P_{\text{CdS-CaI}}(t, N_{\text{tr}}, N_{\text{CaI}})$. The master equation for $P_{\text{CdS-CaI}}(t, N_{\text{tr}}, N_{\text{CaI}})$ is

$$\frac{dP_{\text{CdS-CaI}}(t, N_{\text{tr}}, N_{\text{CaI}})}{dt} = -(k_0 + k_{\text{tr}}N_{\text{tr}} + k_{\text{ET}}N_{\text{CaI}})P_{\text{CdS-CaI}}(t, N_{\text{tr}}, N_{\text{CaI}}). \quad (\text{Eq. S9})$$

Just like the model discussed above, the term $k_{\text{ET}}N_{\text{CaI}}$ is the probability per unit time to decay to any of the N_{CaI} enzymes on the NR. The solution to Eq. S9 is

$$P_{\text{CdS-CaI}}(t, N_{\text{tr}}, N_{\text{CaI}}) = P_{\text{CdS-CaI}}(t_0, N_{\text{tr}}, N_{\text{CaI}})e^{-(k_0+k_{\text{tr}}N_{\text{tr}}+k_{\text{ET}}N_{\text{CaI}})(t-t_0)}. \quad (\text{Eq. S10})$$

Again, factorizing the initial conditions, $P_{\text{CdS-CaI}}(t_0, N_{\text{tr}}, N_{\text{CaI}}) = P_{\text{CdS-CaI}}(t_0)$. Assuming that the coverage of both enzymes and traps is low and that they do not interact, i.e., each is at a fixed chemical potential, the joint probability factorizes, $P(N_{\text{tr}}, N_{\text{CaI}}) = P(N_{\text{tr}})P(N_{\text{CaI}})$. Using the same model for each species as above,

$$P(N_{\text{tr}}) = \frac{\langle N_{\text{tr}} \rangle^{N_{\text{tr}}} e^{-\langle N_{\text{tr}} \rangle}}{N_{\text{tr}}!} \quad (\text{Eq. S11})$$

$$P(N_{\text{CaI}}) = \frac{\langle N_{\text{CaI}} \rangle^{N_{\text{CaI}}} e^{-\langle N_{\text{CaI}} \rangle}}{N_{\text{CaI}}!}. \quad (\text{Eq. S12})$$

Where $\langle N_{\text{CaI}} \rangle$ and $\langle N_{\text{tr}} \rangle$ are the average numbers of enzyme attached to the CdS NR and traps in the NR, respectively, at thermal equilibrium. $P_{\text{CdS-CaI}}(t)$ is therefore

$$P_{\text{CdS-CaI}}(t) = \sum_{N_{\text{CaI}}=0}^{\infty} \sum_{N_{\text{tr}}=0}^{\infty} P(N_{\text{CaI}})P(N_{\text{tr}})P_{\text{CdS-CaI}}(t, N_{\text{tr}}, N_{\text{CaI}}) \quad (\text{Eq. S13})$$

$$= P_{\text{CdS-CaI}}(t_0) e^{-k_0 t} \left[\sum_{N_{\text{tr}}=0}^{\infty} P(N_{\text{tr}}) e^{-k_{\text{tr}} N_{\text{tr}} t} \right] \left[\sum_{N_{\text{CaI}}=0}^{\infty} P(N_{\text{CaI}}) e^{-k_{\text{ET}} N_{\text{CaI}} t} \right] \quad (\text{Eq. S14})$$

$$= P_{\text{CdS-CaI}}(t_0) e^{-k_0(t-t_0)} [\exp\{\langle N_{\text{tr}} \rangle (e^{-k_{\text{tr}}(t-t_0)} - 1)\}] [\exp\{\langle N_{\text{CaI}} \rangle (e^{-k_{\text{ET}}(t-t_0)} - 1)\}] \quad (\text{Eq. S15})$$

$$= P_{\text{CdS-CaI}}(t_0) \exp\{-k_0(t-t_0) + \langle N_{\text{tr}} \rangle (e^{-k_{\text{tr}}(t-t_0)} - 1) + \langle N_{\text{CaI}} \rangle (e^{-k_{\text{ET}}(t-t_0)} - 1)\} \quad (\text{Eq. S16})$$

Again, as we did in going from Eq. S7 to Eq. S8, we replace $P(t_0)$ in favor of the amplitude, $a_{\text{CdS-CaI}}$:

$$P_{\text{CdS-CaI}}(t) = a_{\text{CdS-CaI}} \exp\{-k_0 t + \langle N_{\text{tr}} \rangle (e^{-k_{\text{tr}} t} - 1) + \langle N_{\text{CaI}} \rangle (e^{-k_{\text{ET}} t} - 1)\} \quad (\text{Eq. S17})$$

VI. Fluctuations in both numbers and intrinsic rate constants for traps and CaI

Here we derive an equation for the survival probability in the presence of fluctuations for the intrinsic rate constants. Fluctuations in the intrinsic rate constants can occur when there are additional sources of disorder in the system beyond the number fluctuations modeled above. For example, distributions in distances between the enzyme and the NR or conformational fluctuations of the enzyme might influence electron transfer rates. In this section we derive the expression for the survival probability for electron trapping when there are fluctuations in the trapping rates. Suppose there are N_{tr} traps in a NR and that the rate constant for each trap is a random variable chosen from some distribution, $k_i = k_{\text{tr}} + \delta_i$, where k_{tr} is the mean of the distribution and δ_i is the fluctuation away from the mean for a given trap, i . The distribution function for each δ_i , $p(\delta_i)$, in the set $\{\delta\} = (\delta_1, \dots, \delta_{N_{\text{tr}}})$ is identical and has finite first and second moments.

The master equation for the survival probability $P_{\text{CdS}}(t, N_{\text{tr}}, \{\delta\})$ is

$$\frac{dP_{\text{Cds}}(t, N_{\text{tr}}, \{\delta\})}{dt} = - \left(k_0 + k_{\text{tr}} N_{\text{tr}} + \sum_{i=1}^{N_{\text{tr}}} \delta_i \right) P_{\text{Cds}}(t, N_{\text{tr}}, \{\delta\}), \quad (\text{Eq. S18})$$

which is the survival probability for a given N_{tr} and a given realization of the random variable $\{\delta\}$. Solving the differential equation, and again omitting t_0 and replacing $P_{\text{Cds}}(t_0, N_{\text{tr}}, \{\delta\})$ in favor of the amplitude $P_{\text{Cds}}(t_0)$ gives

$$P_{\text{Cds}}(t, N_{\text{tr}}, \{\delta\}) = P_{\text{Cds}}(t_0) e^{-(k_0 + k_{\text{tr}} N_{\text{tr}} + \sum_{i=1}^{N_{\text{tr}}} \delta_i)t} \quad (\text{Eq. S19})$$

Because the initial condition is independent of N_{tr} , it must also be independent of the values for the intrinsic rate constants. Thus, for a given N_{tr} we can average over the fluctuations in the intrinsic rates first, and then average over the number fluctuations,

$$\langle e^{-\sum_{i=1}^{N_{\text{tr}}} \delta_i t} \rangle = \int_{-k_{\text{tr}}}^{\infty} \prod_{i=1}^{N_{\text{tr}}} d\delta_i p(\delta_i) e^{-\sum_{i=1}^{N_{\text{tr}}} \delta_i t}, \quad (\text{Eq. S20})$$

$$= \int_{-k_{\text{tr}}}^{\infty} \prod_{i=1}^{N_{\text{tr}}} d\delta_i p(\delta_i) e^{-\delta_i t}, \quad (\text{Eq. S21})$$

$$= \left[\int_{-k_{\text{tr}}}^{\infty} d\delta p(\delta) e^{-\delta t} \right]^{N_{\text{tr}}}, \quad (\text{Eq. S22})$$

$$= \hat{p}(t)^{N_{\text{tr}}}. \quad (\text{Eq. S23})$$

The simplification from Eq. S21 to Eq. S22 comes from the fact that all δ_i are independent, identically distributed random variables chosen from the same distribution. $\hat{p}(t)$ in Eq. S23 is the moment generating function for the distribution of trapping rate fluctuations, $\hat{p}(t) = \int_{-k_{\text{tr}}}^{\infty} d\delta p(\delta) e^{-\delta t}$. Finally, averaging over the Poisson distribution in N_{tr} gives the survival probability in the presence of both sources of fluctuations,

$$P_{\text{Cds}}(t) = \sum_{N_{\text{tr}}=0}^{\infty} P(N_{\text{tr}}) P_{\text{Cds}}(t, N_{\text{tr}}, \delta), \quad (\text{Eq. S24})$$

$$= P_{\text{Cds}}(t_0) \sum_{N_{\text{tr}}=0}^{\infty} P(N_{\text{tr}}) e^{-k_0 t} e^{-k_{\text{tr}} N_{\text{tr}} t} \langle e^{-\sum_{i=1}^{N_{\text{tr}}} \delta_i t} \rangle, \quad (\text{Eq. S25})$$

$$= P_{\text{Cds}}(t_0) e^{-k_0 t} e^{-\langle N_{\text{tr}} \rangle t} \sum_{N_{\text{tr}}=0}^{\infty} \frac{[\langle N_{\text{tr}} \rangle e^{-k_{\text{tr}} t} \hat{p}(t)]^{N_{\text{tr}}}}{N_{\text{tr}}!}, \quad (\text{Eq. S26})$$

which upon replacing $P_{\text{CdS}}(t_0)$ with a_{CdS} yields the final result

$$P_{\text{CdS}}(t) = a_{\text{CdS}} \exp\{-k_0 t + \langle N_{\text{tr}} \rangle (e^{-k_{\text{tr}} t} \hat{p}(t) - 1)\}. \quad (\text{Eq. S27})$$

To gauge the importance of intrinsic rate fluctuations, we approximate $\hat{p}(t)$ at the level of the second cumulant,

$$\hat{p}(t) \approx e^{\frac{\langle \delta^2 \rangle}{2} t^2}. \quad (\text{Eq. S28})$$

Including $\langle \delta^2 \rangle$ in the model functions leads to a negligible decrease in the reduced chi-square value (2% decrease) without appreciably changing the other fit parameters. Therefore, $\langle \delta^2 \rangle$ is a statistically insignificant parameter and the TA data are insensitive to fluctuations in the intrinsic rates.

A similar derivation for CdS–CaI complexes gives

$$P_{\text{CdS-CaI}}(t) = a_{\text{CdS-CaI}} \exp\{-k_0 t + \langle N_{\text{tr}} \rangle (e^{-k_{\text{tr}} t} \hat{p}_{\text{tr}}(t) - 1) + \langle N_{\text{CaI}} \rangle (e^{-k_{\text{ET}} t} \hat{p}_{\text{ET}}(t) - 1)\}, \quad (\text{Eq. S29})$$

where $\hat{p}_{\text{tr}}(t)$ and $\hat{p}_{\text{ET}}(t)$ are the moment generating functions for the distributions in trapping and ET rate fluctuations, $p(\delta_{\text{tr}})$ and $p(\delta_{\text{ET}})$, respectively.

Using the second cumulant approximation $\hat{p}_{\text{ET}}(t) \approx e^{\langle \delta_{\text{ET}}^2 \rangle t^2 / 2}$, including fluctuations in the rates for ET does not statistically improve the fit (reduced chi-squared decreases by 0.05%), indicating that a model with one representative value of k_{ET} is sufficient to describe the TA data reported here.

VII. Error analysis for k_0 , $\langle N_{\text{tr}} \rangle$, k_{tr} , $\langle N_{\text{CaI}} \rangle$ and k_{ET}

To determine the fit parameters k_0 , $\langle N_{\text{tr}} \rangle$, k_{tr} , $\langle N_{\text{CaI}} \rangle$ and k_{ET} and their uncertainties, we employed the bootstrapping Monte Carlo method.¹² Distributions for model parameters and their correlations come from generating 10,000 synthetic datasets by resampling the original data with replacement and performing nonlinear least squares fits for each set. The fit parameters that minimize the chi-square value from this process are distributed around the parameters of best fit (Table 1). Joint parameter distributions for particular pairs appear in Fig. S4.

Bootstrapping data indicate strong correlations between fit parameters as one might expect from such a nonlinear, multi-parameter data model. These correlations imply that standard error estimates of each parameter taken individually are insufficient to represent the uncertainties for all parameters simultaneously. The uncertainties reported for the fit parameters in Table 1 include covariances between parameters and represent the 95% confidence in the multidimensional parameter space.¹²

Joint probability distributions for fitting parameters

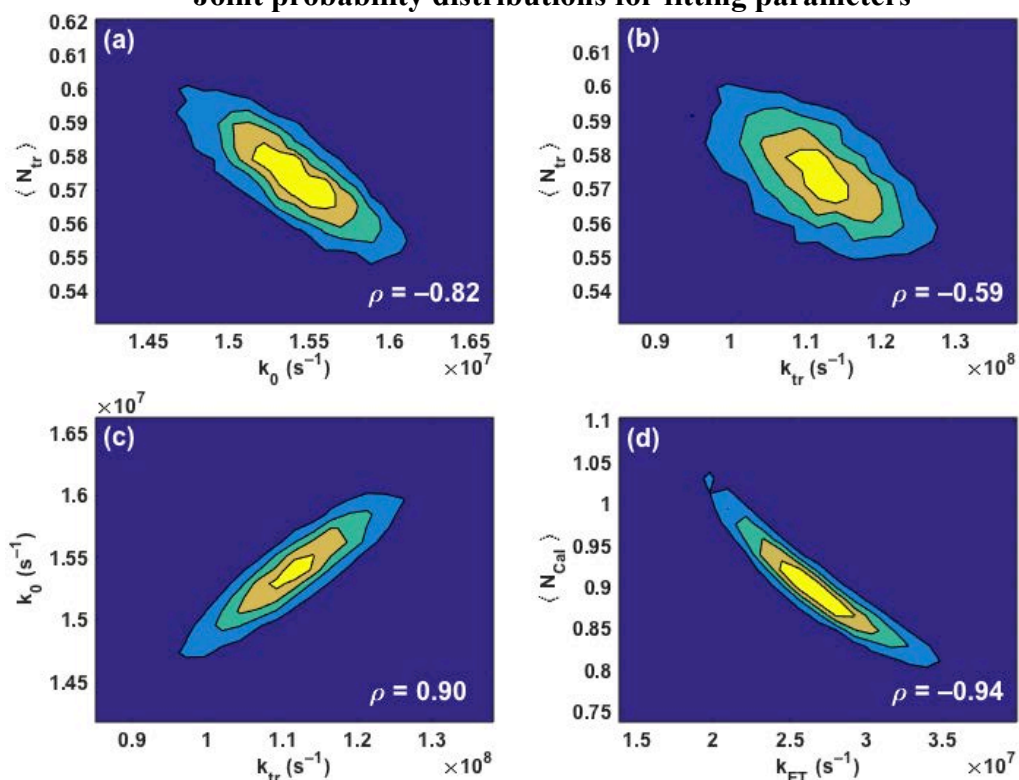


Fig. S4. Joint probability distributions for parameter pairs generated by bootstrapping Monte Carlo resampling. Parameter distributions are shown pairwise for (a) $\langle N_{tr} \rangle$ and k_0 ; (b) $\langle N_{tr} \rangle$ and k_{tr} ; (c) k_{tr} and k_0 , and; (d) $\langle N_{Cal} \rangle$ and k_{ET} . Distributions (a), (b) and (c) were produced from the 0.00:1 data set from Table S1 and (d) was produced from the 1.70:1 data set. Pearson's correlation coefficient for each pair of parameters, ρ , appears in each panel of the figure.

VIII. Kinetic modeling of another CdS-CaI dataset

To assess the reproducibility of fit parameters found in this communication, we apply our analysis to previously published data on the decay kinetics of CdS–CaI complexes.¹³ The CdS NRs used for that data set come from the same synthesis batch as the ones used in the manuscript. The fitting parameters obtained by fitting the data in Fig. S5 to Eqs. 2 and 3 are summarized in Table S1.

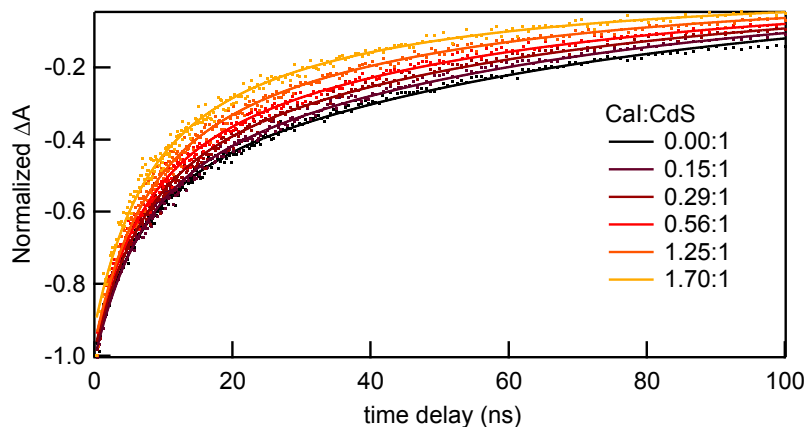


Fig. S5. Band gap TA kinetics of CdS–CaI complexes (dots) for various ratios CaI:CdS and fits to Eq. 3 of the manuscript (solid lines). Ratios listed are the molar ratios upon mixing during sample preparation.

Table S1. Electron decay parameters for another data set of CdS NRs and CdS–CaI complexes

CaI:CdS molar ratio	k_0 (10^7 s $^{-1}$) ^a	$\langle N_{\text{tr}} \rangle$ ^a	k_{tr} (10^8 s $^{-1}$) ^a	$\langle N_{\text{CaI}} \rangle$ ^b	k_{ET} (10^7 s $^{-1}$) ^b
0.00:1	1.54 ± 0.08	0.57 ± 0.03	1.1 ± 0.2	–	–
0.15:1	↓	↓	↓	0.17 ± 0.02	2.2 ± 0.3
0.29:1				0.30 ± 0.02	
0.56:1				0.44 ± 0.03	
1.25:1				0.70 ± 0.04	
1.70:1				0.99 ± 0.05	

^a Values found by fitting CdS NR kinetic trace (Fig. S5) according to Eq. 2.

^b Result of global fit of data in Fig. S5 to Eq. 3 by holding k_0 , k_{tr} , and $\langle N_{\text{tr}} \rangle$ fixed, defining k_{ET} as a global variable between data sets containing CaI, and allowing $\langle N_{\text{CaI}} \rangle$ to vary. Uncertainties associated with each fit parameter are 95% confidence intervals.

The values of k_0 , k_{tr} , and $\langle N_{\text{tr}} \rangle$ in Table S1 are consistent with those in Table 1 within the 95% confidence interval, indicating that the behavior described here is reproducible for CdS NRs made in the same synthesis. The value of k_{ET} obtained from this data set also agrees with that of the data set in the manuscript, within the confidence interval.

IX. QE_{ET} as a function of the intrinsic rate constants

While the QE_{ET} for an individual CdS–CaI complex can be calculated by $\text{QE}_{\text{ET}} = k_{\text{ET}}N_{\text{CaI}}/(k_0 + k_{\text{tr}}N_{\text{tr}} + k_{\text{ET}}N_{\text{CaI}})$, calculation of QE_{ET} for an ensemble requires the inclusion of the distribution in the number traps and adsorbed CaI. This can be done using signal intensities according to¹⁴

$$\text{QE}_{\text{ET}} = 1 - \frac{\int_0^{\infty} dt P_{\text{CdS-CaI}}(t)}{\int_0^{\infty} dt P_{\text{CdS}}(t)} = 1 - \frac{\int_0^{\infty} d(k_0 t) P_{\text{CdS-CaI}}(k_0 t)}{\int_0^{\infty} d(k_0 t) P_{\text{CdS}}(k_0 t)}, \quad (\text{Eq. S30})$$

where $P_{\text{CdS}}(t)$ and $P_{\text{CdS-CaI}}(t)$ are the fits of TA kinetics of CdS NRs to Eq. 2 and CdS–CaI complexes to Eq. 3, respectively.¹⁵ Changing integration variables in the expression for the quantum yield from t to $k_0 t$ as in the second part of Eq. S30 shows that the quantum yield of electron transfer depends only on the ratio of rate constants, so that there are two degrees of freedom and not three for fixed values of $\langle N_{\text{tr}} \rangle$ and $\langle N_{\text{CaI}} \rangle$. That is, $\text{QE}_{\text{ET}}(k_0, k_{\text{tr}}, k_{\text{ET}}) = \text{QE}_{\text{ET}}(k_{\text{tr}}/k_0, k_{\text{ET}}/k_0)$. Fig. S6a shows $\text{QE}_{\text{ET}}(k_{\text{tr}}/k_0, k_{\text{ET}}/k_0)$, evaluated by numerical integration of Eq. S30 for $\langle N_{\text{tr}} \rangle = 0.59$ and $\langle N_{\text{CaI}} \rangle = 1$. QE_{ET} shows a very weak dependence on k_{tr}/k_0 because $\langle N_{\text{tr}} \rangle$ is already very small, so the most important parameter in determining the quantum efficiency for electron transfer is k_{ET}/k_0 .

Because the most important quantity in determining QE_{ET} is k_{ET}/k_0 , increasing k_{ET} , decreasing k_0 , or changing both to increase the ratio increases the quantum efficiency for electron transfer. Fig. S6b shows the predicted values of QE_{ET} as a function of k_{ET}/k_0 , for fixed values of $\langle N_{\text{tr}} \rangle$ and k_{tr} when $\langle N_{\text{CaI}} \rangle = 1$. The circles in Fig. S6a and S6b mark the $\text{QE}_{\text{ET}} = 41\%$ calculated when the values for all parameters take on those that are measured in this communication (Table 1). QE_{ET} saturates to $\approx 63\%$ when $k_{\text{ET}}/k_0 \approx 100$. This is because at $\langle N_{\text{CaI}} \rangle = 1$, 37% of CdS NRs in the sample have no CaI adsorbed and therefore do not undergo ET.

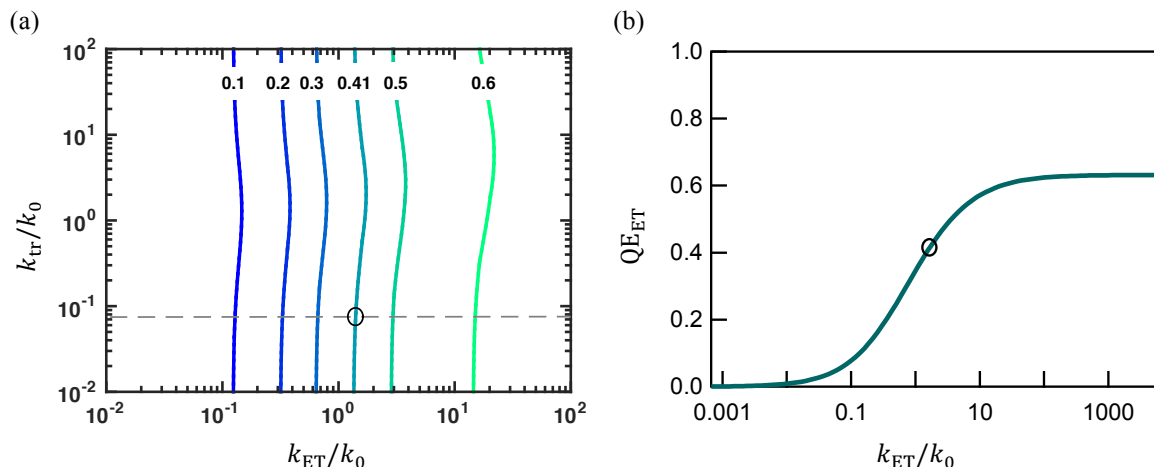


Fig. S6. Quantum efficiency of electron transfer, QE_{ET} , for $\langle N_{\text{CaI}} \rangle = 1$. (a) Contour plot of QE_{ET} as a function of k_{tr}/k_0 and k_{ET}/k_0 . Contour lines of constant QE_{ET} , where the labels denote the values of the contours, run roughly parallel to the y-axis indicating that the quantum yield for electron transfer depends very weakly on k_{tr}/k_0 when $\langle N_{\text{tr}} \rangle = 0.59$. The gray dashed line in (a) marks the slice of the data plotted in (b). The circle indicates the point in parameter space where the CdS–CaI system currently lies. $QE_{\text{ET}} = 41\%$ when k_0 , $\langle N_{\text{tr}} \rangle$, k_{tr} and k_{ET} take on the values presented in Table 1 ($k_{\text{tr}}/k_0 = 7.3$ and $k_{\text{ET}}/k_0 = 1.6$). (b) QE_{ET} as a function of k_{ET}/k_0 where k_0 , $\langle N_{\text{tr}} \rangle$ and k_{tr} values given in Table 1. This trace corresponds to the gray dashed line in (a). The circle shows the point where $QE_{\text{ET}} = 41\%$ ($k_{\text{ET}}/k_0 = 1.6$), which is the QE_{ET} we find from the fits to the TA data (Table 1).

X. References

1. P. Peng, B. Sadtler, A. P. Alivisatos and R. J. Saykally, *J Phys Chem C*, 2010, **114**, 5879-5885.
2. K. A. Brown, M. B. Wilker, M. Boehm, G. Dukovic and P. W. King, *J Am Chem Soc*, 2012, **134**, 5627-5636.
3. H. W. Tseng, M. B. Wilker, N. H. Damrauer and G. Dukovic, *J Am Chem Soc*, 2013, **135**, 3383-3386.
4. C. A. Schneider, W. S. Rasband and K. W. Eliceiri, *Nat Methods*, 2012, **9**, 671-675.
5. L. Amirav and A. P. Alivisatos, *J Phys Chem Lett*, 2010, **1**, 1051-1054.
6. P. W. King, M. C. Posewitz, M. L. Ghirardi and M. Seibert, *J Bacteriol*, 2006, **188**, 2163-2172.
7. V. I. Klimov, *Annu Rev Phys Chem*, 2007, **58**, 635-673.
8. K. Wu, W. Rodríguez-Córdoba and T. Lian, *J Phys Chem B*, 2014.
9. M. B. Wilker, K. E. Shinopoulos, K. A. Brown, D. W. Mulder, P. W. King and G. Dukovic, *J. Am. Chem. Soc.*, 2014, **136**, 4316-4324.
10. S. Sadhu, M. Tachiya and A. Patra, *J Phys Chem C*, 2009, **113**, 19488-19492.
11. N. G. VanKampen, *North-Holl Pers Libr*, 2007, 1-463.
12. W. H. Press, S. A. Teukolsky, W. T. Vetterling and B. P. Flannery, *Numerical Recipes: The Art of Scientific Computing*, 3rd edn., Cambridge University Press, 2007.
13. M. B. Wilker, K. E. Shinopoulos, K. A. Brown, D. W. Mulder, P. W. King and G. Dukovic, *J Am Chem Soc*, 2014, **136**, 4316-4324.
14. J. R. Lakowicz, *Principles of Fluorescence Spectroscopy*, Springer, New York, 2006.
15. S. Sadhu, M. Tachiya and A. Patra, *J. Phys. Chem. C*, 2009, **113**, 19488-19492.